24th ABCM International Congress of Mechanical Engineering
December 3-8, 2017, Curitiba, PR, Brazil

COBEM-2017-0249
MODES I AND II FATIGUE INDUCED DELAMINATION IN CO- CURED COMPOSITE STRUCTURAL JOINTS

Francis M. González R.
Felipe P. Garpelli
Instituto Tecnológico de Aeronáutica, São José dos Campos, SP, 12228-900, Brazil
francismgonzalezr@gmail.com; felipegarpelli92@yahoo.com.br

Nubia N. A. Silveira
Instituto Tecnológico de Aeronáutica
nubianale@gmail.com

Rita de Cássia M. Sales
Instituto Tecnológico de Aeronáutica
Faculdade de Tecnologia de São José dos Campos Prof. Jessen Vidal, São José dos Campos, Brazil
rita.sales@fatec.sp.gov.br

Marcos Y. Shiino
Universidade Estadual Paulista - Instituto de Ciência e Tecnologia, Departamento de Engenharia Ambiental, São José dos Campos, SP, 12247-004, Brazil
marcosshiino@yahoo.com.br

Mariano A. Arbelo
Instituto Tecnológico de Aeronáutica
marbelo@ita.br

Mauricio V. Donadon
Instituto Tecnológico de Aeronáutica
donadon@ita.br

Abstract. *An experimental procedure was developed to characterize fatigue delamination growth in co-cured composite joints. No-growth criterion was used to guarantee that crack growth does not reach an unsafe size during the lifetime of the component. The tests were performed for Modes I and II loading configurations, using the double cantilever beam (DCB) and the three-point bend end notched flexure (3-ENF) specimens respectively. The DCB tests were carried out following the ASTM D6115 procedure. There is no standard test procedure for conducting Mode II fatigue delamination tests. The ENF test was chosen based in previous works available in the literature and the ASTM D 7905. Information from previous quasi-static tests (using specimens with the same material batch and geometry) was used to define the load and displacement values for various G-levels, leading to a relationship between the maximum strain energy release rate (SERR-*G_{max}*) and the number of cycles associated with the onset of delamination growth (G–N curve). Experimental results show that the co-cured joints exhibit an overall better fatigue performance in pure mode II loading. Additionally, SEM fractography studies were performed to both loading modes in order to analyze their morphology surfaces. The testing procedures used in this study, and the associated test results will be useful to develop robust criteria based on safe life design in composite aerostructures.*

Keywords: *Fatigue delamination growth, Mode I and II, Double cantilever beam, End notched flexure, strain energy release rate.*

1. INTRODUCTION

Nowadays, laminated composites based on fiber-reinforced polymer have been extensively used under cyclic conditions in aeronautical structures, due to their high strength to weight ratio (Nwose *et al.*, 2003; Arguelles *et al.*, 2011). Composite materials consist of two or more materials combined on a macroscopic scale to produce properties that cannot be achieved with any of the constituents independently (Reddy, 2000; Isaac *et al.*, 1994). Composite laminates generally are materials with fibers of high modulus and strength, embedded in a polymer matrix with distinct interfaces between them (Reddy, 2000; Mallick, 2007). Subsequently, fibers carry the principal loadings, while the matrix maintains the fibers together in the desirable position and orientation, acting as a load transferring medium and protecting them from environmental weathering (Reddy, 2000; Mallick, 2007).

The adhesive bonding technique has gained importance over conventional joining methods (welding, bolting and riveting) used in aerospace structures (Budhe *et al.*, 2017; Hu *et al*, 2013; Shenoy *et al.*, 2013). It worth mentioning some advantages as high strength and stiffness to weight ratio, design flexibility, damage tolerance, more uniform stress distribution on the bonded area, reduction of stress concentrations and high fatigue resistance (Budhe *et al.*, 2017; Hu *et al.*, 2013; Shenoy *et al*, 2013; Fernandes *et al.*, 2016). Currently, there are three main manufacturing processes for joining composite parts in the aeronautical industry: co-curing, co-bonding and secondary bonding method [6]. The co-bonding process is performed when the adherend is cured with the adhesive and the secondary bonding process is when the adhesive layer is cured between two pre-cured plates (Budhe *et al.*, 2017). The co-cured joints used in this work are composed of two prepreg plates joined and cured together, without the addition of any adhesive film besides its own resin matrix.

The failure modes, commonly observed in composite materials, can be divided into four different modes of damage: transverse matrix cracks, fiber fracture, fiber-matrix interface damages and delamination (Nwose *et al.*, 2003). Delamination is responsible for 60% of structural failures in composite laminates whilst in service (Charalambous *et al.*, 2015). This issue relates to interlaminar cracks that usually originated at interlaminar stress concentrations such as free edges, ply drops, joints, etc. (Andersons *et al.*, 2004). When subjected to cyclic loads, these elements are susceptible to interlaminar cracks that propagate throughout the laminate, leading to degradation of structural integrity and overall failure (Andersons *et al.*, 2004).

Interlaminar crack propagations can occur under one of the following pure modes: the opening mode (Mode I), the sliding mode (Mode II) and the tearing mode (Mode III), or a combination of them (Maillet *et al.*, 2015; Jones *et al.*, 2014; Carrecas *et al.*, 2017). For Mode I fatigue induced delamination tests, the ASTM standard recommends the use of the Double Cantilever Beam (DCB) specimens (Maillet *et al.*, 2015; Carreras *et al.*, 2017). Currently, there is no ASTM standard for conducting Mode II fatigue delamination tests (Carreras *et al.*, 2017; O´Brien *et al.*, 2010).

In laminate composites, the three and four point bend of end-notched flexure test set-ups (3-ENF and 4-ENF, respectively) are generally used for the determination of the Mode II critical interlaminar fracture toughness (G_{IIc}) (Sun and Davidson, 2006). Carreras *et al*. (2017) reported that 3-ENF is the most widely used testing configuration for Mode II fatigue induced delamination tests performed under displacement control and sinusoidal load. In fact, O'Brien *et al*. (2010) establish that this set up is currently under review by ASTM as a potential standard test method. Sun and Davidson (2006) show that the diameter of the loading rollers typically used in flexural testing setups causes in both cases inherent geometric nonlinearities. However, the effect of these nonlinearities is more pronounced in the 4-ENF than the 3-ENF, where significantly increases the coefficient of friction along the crack plane. The authors concluded that the 3-ENF provided more reliable results for Mode II fatigue induced delamination tests. Carreras *et al.* (2017) also confirmed that the 4-ENF test is not preferred due to frictional effects. Davidson *et al.* (2017) highlighted the importance of a stiff test fixture and loading frame for these types of tests. Their work shows that a standard three-point bending fixture with high stiffness is relatively straightforward and that the test results are essentially equal to expected ones. Furthermore, it is much more difficult to produce a stiff fixture for the 4-ENF. Based on these findings the 3-ENF configuration was chosen for the Mode II fatigue delamination tests presented in this work.

The objective of this paper is to analyze and discuss the results of the onset fatigue induced delamination growth tests in Mode I and II in co-cured bonded joints, as well as to outline the procedures to conduct the tests based on quasi-static delamination results.

2. EXPERIMENTAL PROCEDURE

The composite material used in this study was manufactured from T800 fibers embedded in a 3900-2C Toray® prepreg UD resin. All the specimens have a thin teflon film inserted in the mid-plane that acts as a crack starter. The lay-up of DCB and 3-ENF specimens used were $[0^{\circ}]_{26}$. The ASTM D6115 (2004), standard test method for Mode I fatigue delamination growth, recommends a minimum of 6 specimens for the development of a strain energy release rate versus number on cycles (G-N) curve in the DCB tests. The same consideration was taken for 3-ENF configuration.

The specimen's dimensions were: length (L) 175.5 mm, width (B) 20 mm, thickness (h) 4.9 mm, and initial delamination length (a_0) 50 mm (Figure 1.a). Following the ASTM D7905 (2014) standard for the 3-ENF quasi-static tests, the distance between the support rollers and the loading roller was 50 mm (L_r) (Figure 1.b). When a sample is placed in the test machine, it is important to guarantee a distance of 30 mm between the center of the left support roller and the end of the insert (a_r). The rollers' diameter is 10 mm (Figure 1.b).

For both testing configurations, the number of cycles associated with the onset of the delamination growth for a given strain energy release rate ratio (G-level) was defined based on a reduction of 5% in the maximum load measured at the first cycle N=1 (ASTM D6115, 2004). Table 1 presents the average values of the modulus of elasticity (E), compliance ($|\Delta|_{av}$) and the critical interlaminar fracture toughness for Mode I (G_{Ic}) and II (G_{IIc}) obtained from previous quasi-static tests carried out using samples of the same batch (Brito, 2017). The specimens were cycled under displacement control at a frequency of 5 Hz (to avoid heating effects) (ASTM D6115, 2004).

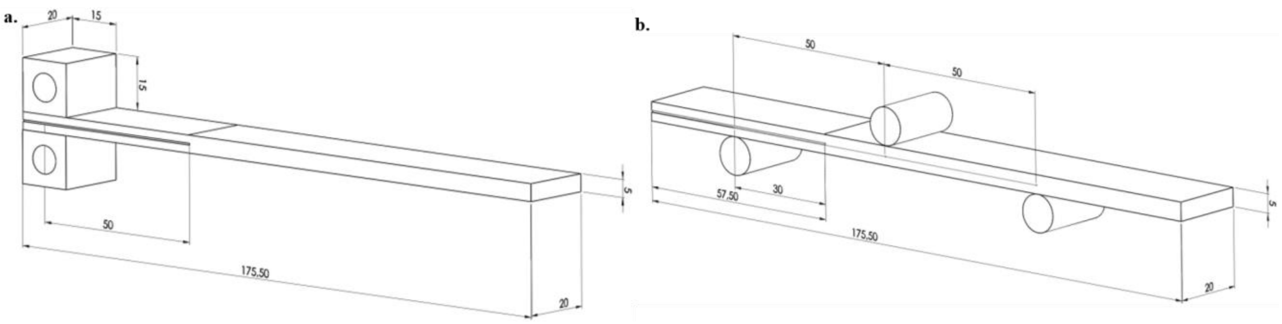

Figure 1. Isometric view and dimensions of (a) the DCB and (b) the 3-ENF specimens (dimensions are in mm).

Table 1. Average values from de quasi-static test performed by Brito (2017).

	E [Mpa]	**G_{Ic} [N/mm]**	**G_{IIc} [N/mm]**	**$\|\Delta\|_{av}$**
Average	92094.3	0.095	0.798	8,5526

2.1. Mode I fatigue tests

The DCB fatigue tests were performed using a servo-hydraulic MTS testing machine (370.10) with a load cell of 100 lb (≈445 N). These tests were carried out in the Aerospace structures laboratory at Instituto Tecnológico de Aeronáutica (ITA). Two load blocks were bonded to the upper and lower surface of the cracked end side of each specimen (Figure 1.a and 2).

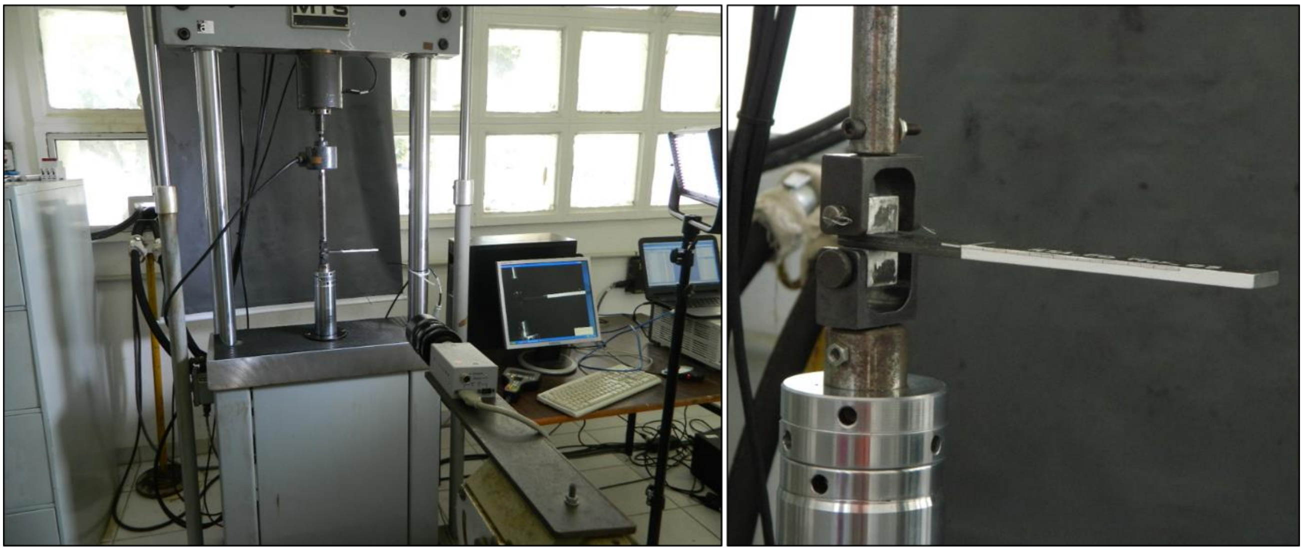

Figure 2. Mode I fatigue induced delamination test setup.

For DCB tests, Eq. (1), Eq. (2) and Eq. (3) were used to obtain a relationship between the critical load (P_{cr}) and critical displacement (δ_{cr}) for delamination onset (ASTM D6115, 2004):

$$P_{cr} = \frac{1}{a_0}\sqrt{(G_{IC} BEI_H)} \tag{1}$$

$$\delta_{cr} = \frac{(P_{cr} a_0{}^3)}{3(EI_H)} \tag{2}$$

$$I_H = \frac{(Bh^3)}{96} \tag{3}$$

Where I_H is the cross section moment of inertia of half of the sample (h/2).

For Mode I fatigue characterization, ASTM D6115-97 (2004) standard recommends a relation G_{Imax}/G_{Icr} =50% (G-level) to start with, based on Eq. (4):

$$\frac{\delta_{max}^2}{\left[\delta_{cr}\right]_{max}^2} = \frac{G_{Imax}}{G_{IC}} = 0{,}50 \tag{4}$$

$$\rightarrow \delta_{max} = \left[\delta_{cr}\right]_{max} \sqrt{0{,}50}$$

With δ_{max} calculated and considering a R-ratio ($\delta_{max}/\delta_{min}$) of 0.1, it was possible to obtain the minimum (δ_{min}) and mean (δ_{mean}) displacement, thus providing all the required parameters to initiate the test. To complete a G–N curve, several values of G_{Imax} were tested for different G-levels. From the values of δ_{max} and P_{max} at N=1 and the average of compliance constant ($|\Delta|_{av}$), G_{Imax} was calculated for each specimen by using the beam theory correction (ASTM D6115, 2004):

$$G_{Imax} = \frac{3(P_{max}\delta_{max})}{2B(a + |\Delta|_{av})} \tag{5}$$

2.2. Mode II fatigue tests

All the 3-ENF fatigue tests were performed at the Instituto de Pesquisas Tecnológicas (IPT), in S.P., Brazil. Using a servo-hydraulic MTS testing machine with a load cell of 15 kN (Figure 3). Before the test initiation, the standard recommends a preload application (in these work of 10 N) to ensure that the collected data is not affected by any initial nonlinearity.

To obtain the relationship between the load (P) and displacement (δ) of the 3-ENF tests an analytical model was employed. Equation 6 describes this relation before the propagation of the crack (the linear portion) and Equation 7 describes it at the crack propagation regime. Equation 8 defines the cross section moment of inertia of the beam.

$$\delta = \frac{P(2L_r{}^3 + 3a_r{}^3)}{12EI} \tag{6}$$

$$\delta = \frac{P}{12EI}\left(2L_r{}^3 + \frac{(8G_{IIC}BEI)^{3/2}}{\sqrt{3}P^3}\right) \quad \text{for } a < L_r \tag{7}$$

$$I = \frac{(Bh^3)}{12} \tag{8}$$

From the model above, the critical load (P_{cr}) and displacement (δ_{cr}) was achieved at the intersection of both curves. As in DCB tests, for each G-Level the parameters required to initiate a test are: the minimum (δ_{min}), mean (δ_{mean}) and maximum (δ_{max}) displacement, which are calculated by Eq. (4). Finally, from the values of δ_{max} and P_{max} at N=1, G_{IImax} can be calculated using Eq. (9) (Donadon and Faria, 2016):

$$G_{IImax} = \frac{3(P_{\max}^2 a_r^2)}{8(BEI)} \tag{9}$$

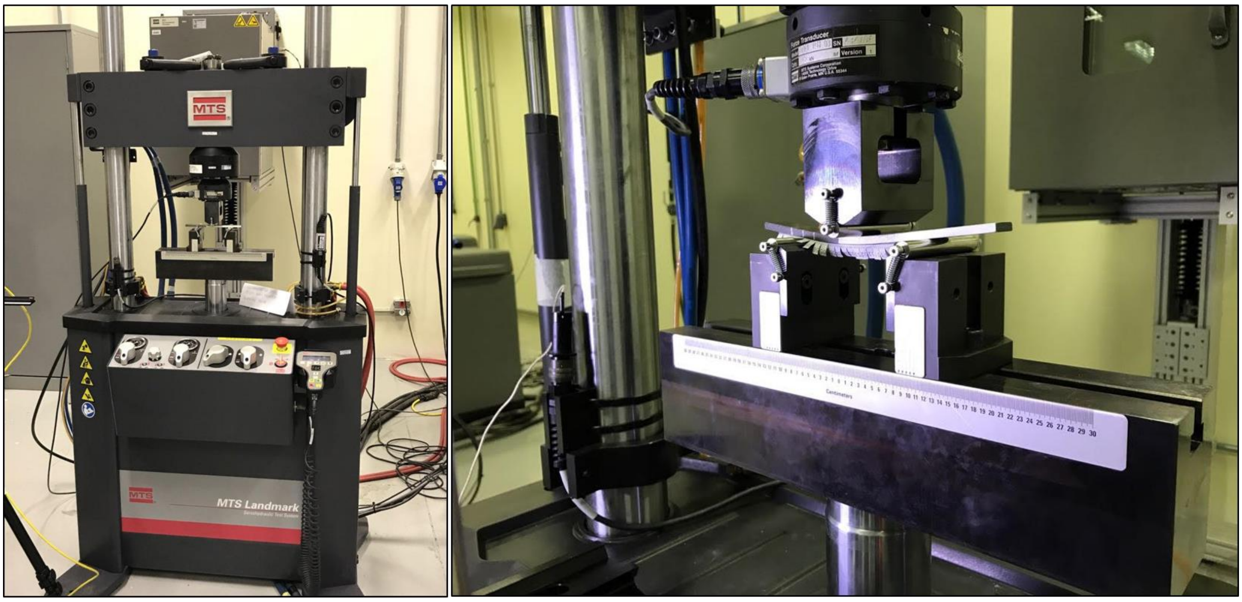

Figure 3: Mode II fatigue induced delamination test setup.

3. TEST RESULTS

The number of cycles for crack initiation in each energy level is shown in Figure 4, where the orange curve represents the different energies for Mode II initiation, and the yellow curve represents the energies for Mode I initiation.

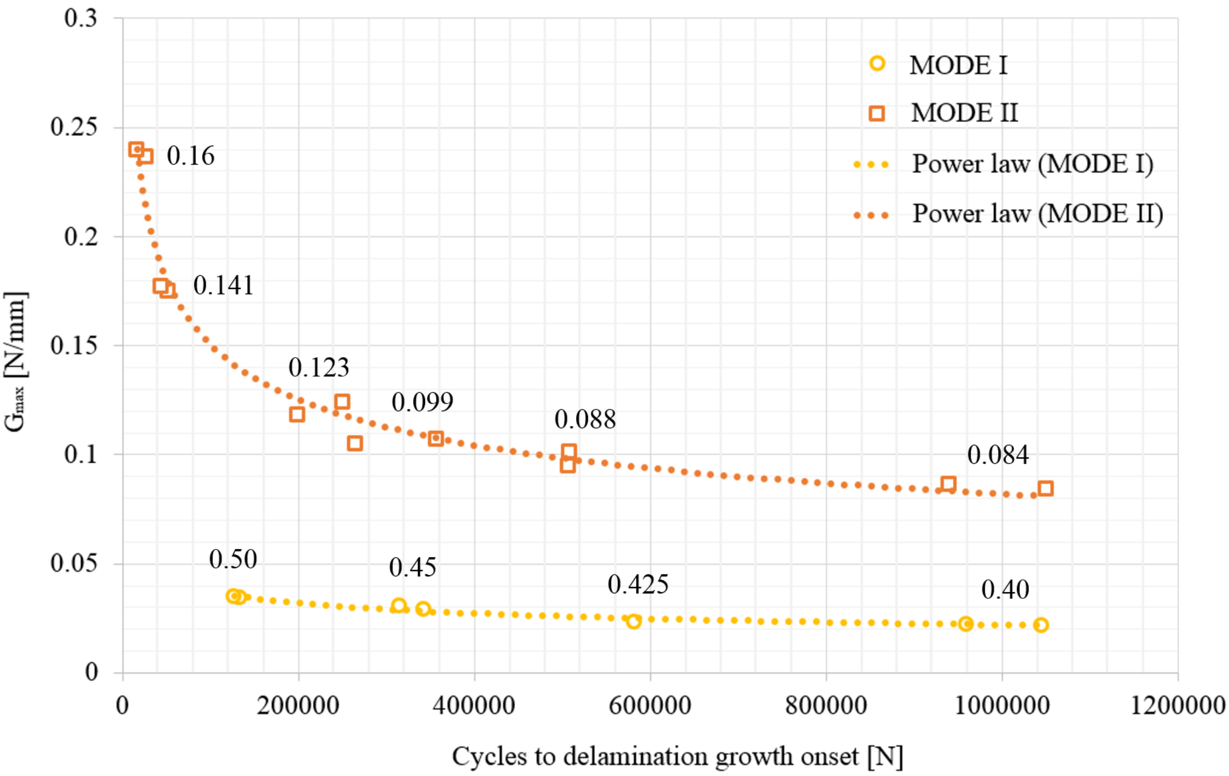

Figure 4. Variation of onset fatigue life for different G-Levels in Mode I and II loading configurations.

Figure 4 shows the G-N curves for the DCB and 3-ENF tests. For Mode I configuration seven specimens were tested. Values of G_{Imax} were subsequently determined for decreasing G-Level percentage as follows: 0.5, 0.45, 0.425 and 0.40 (Table 2). For Mode II twelve specimens were tested. G_{IImax} values were obtained for the following G-Levels:

0.16, 0.141, 0.123, 0.099, 0.088 and 0.084 (Table 3). It is considered that one million cycles with no detectable crack extension provides a reliable threshold value. The DCB tests achieved their threshold energy release rate (10^6 cycles) for a G-level of 0.40, with average value of G_{Imax}= 0.021954 N/mm, while the 3-ENF tests reached it for a G-level of 0.084, with average value of G_{Imax}= 0.084403 N/mm.

Table 2. Fatigue onset test data for the DCB specimens.

Specimen	G-Level	N [cycles]	G_{Imax} [N/mm]
DCB01	0.5	127000	0.035088
DCB02	0.5	134000	0.034319
DCB03	0.45	315000	0.030719
DCB04	0.45	343000	0.028875
DCB05	0.425	581500	0.023396
DCB06	0.40	959000	0.022474
DCB07	0.40	1048000	0.021954

Table 3. Fatigue onset test data for the 3-ENF specimens.

Specimen	G-Level	N [cycles]	G_{IImax} [N/mm]
3-ENF01	0.1601	27500	0.236799
3-ENF02	0.1601	17000	0.239970
3-ENF03	0.1406	51500	0.174815
3-ENF04	0.1406	44500	0.177201
3-ENF05	0.1228	251000	0.124028
3-ENF06	0.1228	199000	0.118382
3-ENF07	0.099	357000	0.106981
3-ENF08	0.099	265500	0.104961
3-ENF09	0.088	506500	0.094910
3-ENF10	0.088	509000	0.101373
3-ENF11	0.084	1050500	0.084403
3-ENF12	0.084	940000	0.086593

O´Brien (1990) suggested that the G-N curve could be describe by linear equation between $10^0 \leq N \leq 10^6$. For the present study, a linear regression did not fit properly to the data. Following Shivakumar *et al.* (2006) and Al-Khudairi *et al.* (2015) a non-linear regression was fit to the data of both fatigue modes (Figure 4) providing a power law relation. For the DCB and 3-ENF set-ups a power law equation fits accurately providing a squared correlation of R^2= 0.96 and R^2= 0.98, respectively:

$$G_{Imax} = 0.05236N^{-0.229}$$

$$G_{IImax} = 3.141N^{-0.264}$$

It can be observed that the co-cured joints used in this work performed better in Mode II in the overall range of stresses analyzed. This behavior could be explained by the usual mechanism of failure (crack propagation) present by this loading configuration (Brito, 2017; Shiino *et al*, 2014). In Mode II, crack propagation occurs as a consequence of the microcracks coalescence. Brito (2017) suggested that these microcracks take place in a damage zone located ahead of the crack tip, thus causing an increase of the surface area related to the crack propagation, consequently, more energy is involved in the process. Anderson (2005) established that the increasing of the fracture toughness is related to the dissipation of this energy in that large damage zone.

4. FRACTOGRAPHY ANALYSES.

A fractography analysis was performed on specimens of both loading modes using a scanning electron microscope (SEM) VEGA3 XMU TESCAN. All the images were taken in the section between teflon film and the resin pocket. The samples were cut in smaller beams leaving enough distance to not affect the area of study. To improve the visualization of the surface morphology, the surface of the specimens were covered with a thin film of gold using a vacuum pump QUORUM-Q150RE5.

Figure 5(a) shows the fractographic lateral view of a Mode I sample. In this image, the carbon fiber and polymeric matrix layers can be observed. Additionally, it is possible to notice the teflon film and the resin rich area produced by the change of thickness between the film and the interlayer. Fig. 5(b) presents a higher magnification of the end of the artificial delamination (Region A). The interface between teflon film and the polymeric matrix presents some microcracks, which is expected in this area due to its function as a crack starter. Furthermore, it was possible to detect some thermoplastic particles located along the resin; these particles have the purpose of improving the fracture toughness of the laminate. In these images, no crack propagation was found.

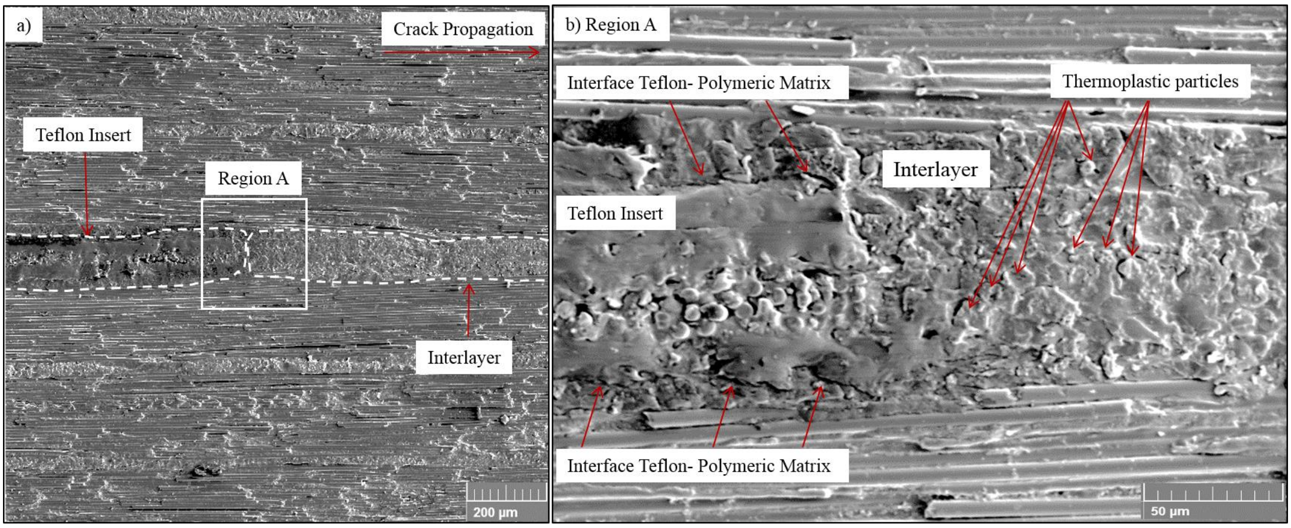

Figure 5. Sample tested under Mode I configuration (a) Side view of the section between teflon film and the resin pocket (Magnification 150x) (b) Interface teflon-Polymeric Matrix and thermoplastic particles (Magnification 1kx).

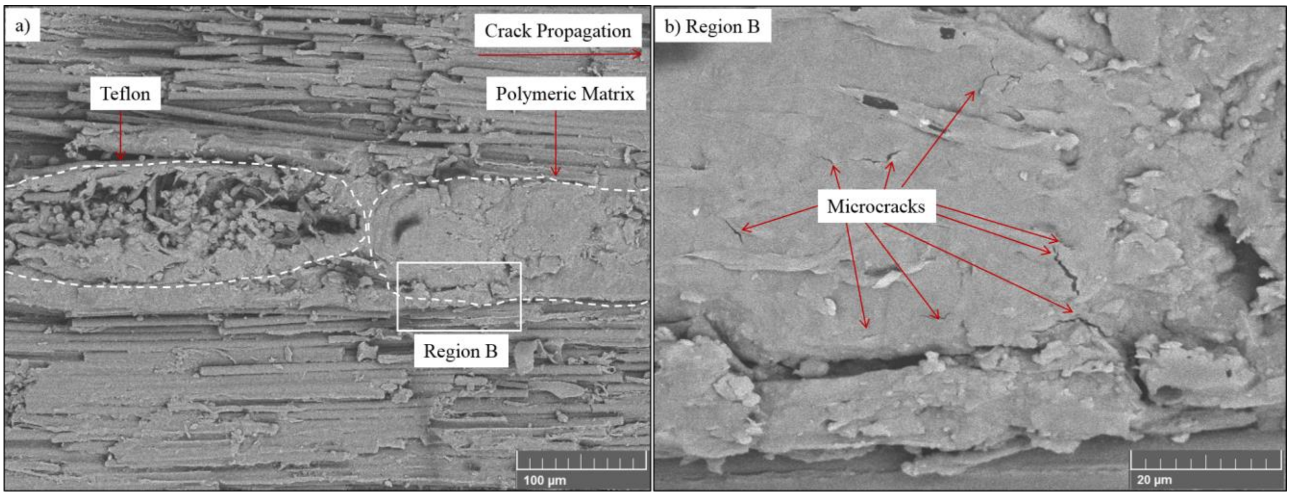

Figure 6. Sample tested under Mode II configuration (a) Side view of the section between teflon film and the resin pocket (Magnification 500x), (b) Microcracks and Thermoplastic particles (Magnification 3kx).

Figure 6 presents the fractographic lateral view of a Mode II specimen. It is noticed in Fig. 6 (a) and more so in Fig.6 (b), that the interface between the teflon film and resin pocket presents a crack initiation, which is probably due to a weak adhesion between these two parts. Additionally the authors observed the presence of several microcracks at the resin rich area, which are typical of the mode II mechanism of failure, as explained in Section 3. This also confirms the higher values of the strain energy release rate obtained in the Mode II tests. It is important to notice that the microcracks did not coalescence

5. CONCLUSIONS

In this paper Mode I (DCB) and Mode II (3-ENF) tests were performed in order to characterize the fatigue delamination growth onset threshold in co-cured composite joints under pure Mode I and II. The three point End Notched Flexure (3-ENF) was chosen as the setup for Mode II fatigue delamination tests due to reduced frictional effects and geometric nonlinearities provided by this configuration in comparison with 4-ENF testing setup. Experimental results show that the co-cured joints investigated in this work exhibit an overall better fatigue performance in pure mode II compared with mode I loading. The values of no-growth threshold energy release rates for mode I and mode II were G_{Imax}= 0.021954 N/mm and G_{IImax}= 0.084403 N/mm, respectively. The experimental results were fitted by a power law type equation. The fractography analyses show thermoplastic particles along the resin of the co-cure joint, these particles could lead to an improved the Mode II strain energy release rate. Microcracks typical of pure mode II were observed in resin rich areas, which may explain the higher energy release rate values found in the 3-ENF tests.

6. ACKNOWLEDGEMENTS

This project is partially supported by the CNPq processes 126346/2016-0, 142761/2016-8, 800319/2016-8, 800392/2016-7 and 300893/2015-9, Capes 1543373, FINEP 0114018300, IPT/FIPT 991914T and FAPESP 2015/16733-2. The authors also acknowledge the LEL-IPT, the Laboratory of Aerospace Structures and Laboratory of Materials and Processes at ITA for providing the infrastructure and equipments needed for the development of this work, Dr Geraldo Maurício Cândido for the in-depth and valuable discussions on the fractography analyses.

7. REFERENCES

Al-Khudairi, O., Hadavinia, H., Waggott, A., Lewis, E., & Little, C., 2015. “Characterising Mode I/Mode II fatigue delamination growth in unidirectional fibre reinforced polymer laminates”. *Materials & Design* (1980-2015), 66, 93-102.

American Society for Testing and Materials (ASTM) D6115-97. 6115-97(11), 2004. “Standard test method for Mode I fatigue delamination growth onset of unidirectional fiber-reinforced polymer matrix composites”. Annual book of ASTM standards, 15.

American Society for Testing and Materials (ASTM) Standard. D7905/d7905m14, 2014. “Standard Test Method for Determination of the Mode II Interlaminar Fracture Toughness of Unidirectional Fiber-Reinforced Polymer Matrix Composites”.

Andersons, J., Hojo, M. and Ochiai, S., 2004. "Empirical model for stress ratio effect on fatigue delamination growth rate in composite laminates*". International Journal of Fatigue*, 26, 597–604.

Anderson, T., 2005. *Fracture Mechanics: Fundamental and Applications*. CRC Press, 3rd edition.

Arguelles, A., Viña, J., Canteli, A. F. and Bonhomme, J., 2011. "Influence of Resin Type on the Delamination behavior of Carbon Fiber Reinforced Composites Under Mode-II Loading". *International Journal of Damage Mechanics*, 20.

Brito, C. B.G., 2017. *Hygrothermal effects on interlaminar fracture toughness of composite joints.* Master dissertation, Instituto tecnológio de aeronáutica – ITA- São José dos Campos, Brazil.

Budhe, S., Banea, M.D., de Barros, S. and da Silva, L.F.M, 2017. "An updated review of adhesively bonded joints in composite materials*". International Journal of Adhesion & Adhesives*, 72, 30–42.

Carreras, L., Renart, J., Turon, A., Costa, J., Essa, Y., & de la Escalera, F. M., 2017. “An efficient methodology for the experimental characterization of Mode II delamination growth under fatigue loading”. *International Journal of Fatigue*, 95, 185-193.

Charalambous, G., Allegri, G., Lander, J. and Hallet, S., 2015. "A cut-ply specimen for the mixed-mode fracture toughness and fatigue characterization of FRPs". *Composites: Part A*, 74, 77–87.

Davidson, B. D., Sun, X., & Vinciquerra, A. J., 2007. “Influences of friction, geometric nonlinearities, and fixture compliance on experimentally observed toughnesses from three and four-point bend end-notched flexure tests”. *Journal of composite materials*, 41(10), 1177-1196.

Donadon, M.V. and Faria, A., 2016. “Analysis and design of composite structures - Fracture mechanics applied to composite laminates” - *Notas de aula MP-206*, volume 6. ITA, 2016.

Fernandes, R., de Moura M. and Moreira R., 2016. "Effect of moisture on pure mode I and II fracture behavior of composite bonded joints". *Composites Part B*, 96, 35-44.

Hu P., Han, X., da Silva, L.F.M. and Li, W.D., 2013. "Strength prediction of adhesively bonded joints under cyclic thermal loading using a cohesive zone model". *International Journal of Adhesion & Adhesives*, 41, 6–15.

Isaac, Daniel and Ishai, Ori, 1994. *Engineering Mechanics of Composite Materials.* Oxford University Press, New York, USA.

Jones R., Stelzer, D. and Brunner, J., 2014. "Mode I, II and Mixed Mode I/II delamination growth in composites". *Composite Structures*, 110, 317–324.

Maillet, I., Michel, L., Souric, F., & Gourinat, Y., 2015. “Mode II fatigue delamination growth characterization of a carbon/epoxy laminate at high frequency under vibration loading”. *Engineering Fracture Mechanics*, 149, 298-312.

Mallick P. K., 2007. *Fiber-Reinforced Composites: Materials, Manufacturing and design.* CRC Press, USA, 3rd edition.

Nwosu, S., Hui, D. and Dutta, P., 2003. "Dynamic mode II delamination fracture of unidirectional graphite/epoxy composites". *Composites: Part B*, 34, 303–316.

O’Brien T. K., 1990. "Towards a damage tolerance philosophy for composite materials and structures". *ASTM Special Technical Publication*, 1059.

O'Brien, T. K., Johnston, W. M., & Toland, G. J., 2010. “Mode II interlaminar fracture toughness and fatigue characterization of a graphite epoxy composite material”.

Reddy, J. N., 2000. *Mechanics of laminated composite plates and shells: theory and analysis*. CRC Press, Florida, USA, 2nd edition.

Shenoy V., Ashcroft, I.A., Critchlow, G.W., Crocombe, A.D., 2010. "Unified methodology for the prediction of the fatigue behaviour of adhesively bonded joints". *International Journal of Adhesion & Adhesives*, 41, 6–15.

Shiino, M., Alderliesten, R., Donadon, M., Voorwald, H. and Cioffi, M., 2014. “Applicability of standard delamination tests (double cantilever beam and end notch flexure) for 5HS fabric-reinforced composites in weft-dominated surface”. *Journal of Composite Materials.*

Shivakumara, K., Chen, H., Abali, F., Le, D. and Davis, C., 2006. “A total fatigue life model for mode I delaminated composite laminates”¨. *International Journal of Fatigue*, 28, 33-42.

Sun, X., & Davidson, B. D., 2006. “Numerical evaluation of the effects of friction and geometric nonlinearities on the energy release rate in three-and four-point bend end-notched flexure tests”. *Engineering fracture mechanics*, 73(10), 1343-1361.

8. RESPONSIBILITY NOTICE

The authors are the only responsible for the printed material included in this paper.